PAPER • **OPEN ACCESS**

The effect of external helical ribs tube on the heat transfer and pressure drop performance for multi - tube heat exchanger

To cite this article: Ruaa N. Talib *et al* 2019 *IOP Conf. Ser.: Mater. Sci. Eng.* **518** 032015

View the article online for updates and enhancements.

IOP ebooks™

Bringing you innovative digital publishing with leading voices to create your essential collection of books in STEM research.

Start exploring the collection - download the first chapter of every title for free.

This content was downloaded from IP address 180.76.149.31 on 20/09/2019 at 08:54

IOP Conf. Series: Materials Science and Engineering **518** (2019) 032015 doi:10.1088/1757-899X/518/3/032015

The effect of external helical ribs tube on the heat transfer and pressure drop performance for multi - tube heat exchanger

Ruaa N. Talib[1], Nabil J. Yasin[1] and Mohammed A. Nasser[1].
[1]Engineering Technical College-Baghdad, Middle Technical University, Baghdad**,** Iraq.
E-mail: eng_ruaanazar@yahoo.com (Ruaa N. Talib)

Abstract. The pressure drop and heat transfer characteristic for cross flow of turbulent air over helical rectangular ribs tubes heat exchanger were studied experimentally and numerically. The study includes the design and manufacturing of four models of multi-tube heat exchangers. Each model has three tubes in a line arrangement. Experiments were performed for Reynolds number range from (7200–31400) using different rib pitch to diameter ratios (P/D=1.3, 1.5 and 1.8) with different ribs pitch angles. The height to diameter ratio of rib (h/D=0.05) and width to diameter ratio is (w/D=2) were fixed. The water flows with different rates inside the tubes with a range of (2, 3, 4, 5, 6 and 7) L/min. Three values for the inlet water temperatures to test tube were used. In the present numerical part, commercial software ANSYS Fluent 16.2 was employed to determine the heat transfer coefficient and pressure drop for the different models of cross flow heat exchangers. The results declared that the average Nusselt number and Pressure drop of the corrugated model has a relatively high different from that of the smooth models. In addition, the experimental and numerical were compared and gave a good agreement between them.

1. Introduction

The heat transfer technique of the heat exchanger augmentation was used to convective heat transfer increasing by thermal resistance reducing of the heat exchangers. Several techniques of heat transfer enhancement that aims to enhance the coefficients of heat transfer and decreasing the pressure drop across the heat exchangers [1]. One of the heat exchange area modifications in order to promote turbulence flow field and increase the heat transfer surface area is the rough surfaces technique on the outside tubes bundles [2]. **[**3**]** presented a numerical study on the thermal stresses and heat transfer that induced by differences of temperature. They using four different types of internally grooved tubes and employed the finite element method to compute the thermal stress fields. Their results showed that the maximum values of the thermal stresses located near the grooved parts. [4] studied experimentally turbulent air flow friction characteristics and heat transfer different grooved geometric shapes (rectangular, trapezoidal and circular). The result shows that the enhancement of heat transfer was 47%, 58% and 63% for rectangular, trapezoidal, circular grooved respectively in comparison with the smooth tube at Re = 38,000 [5] experimentally investigated the heat transfer by convection in a turbulent single-phase flow by using helically corrugated pipes. The results showed that the rib-height to diameter and pitch to diameter ratios has significant effects on the heat transfer enhancement. [6] investigate numerically a turbulent forced convection in a tube with helical ribs. Three-dimensional turbulent flow has been simulated using a finite volume method. The geometric parameters of single start internally ribbed tubes are, rib pitch to diameter ratio and rib height to diameter ratio were considered. It has been shown that the helical ribs have a significant effect on the heat transfer augmentation and pressure drop. [7] studied numerically the effect of the helical oval tube on the flow

Content from this work may be used under the terms of the Creative Commons Attribution 3.0 licence. Any further distribution of this work must maintain attribution to the author(s) and the title of the work, journal citation and DOI.
Published under licence by IOP Publishing Ltd

and heat transfer behaviors inside the tube. The helical oval tubes with nine oval tube pitch ratios and eight oval tube depth ratios were examined in turbulent regime flow. The results showed that the increasing of pitch ratio and decreasing depth ratio are useful to reduce the pressure loss of the tube heat exchanger. [8]investigated the effect of discrete corrugated rib roughened tube on heat transfer and frictional losses under different fluid flow rates with several configurations of corrugated tubes with one, three and five number of gaps respectively were used. The results found that the Nusselt number enhancement is 2.73 and the friction factor is 2.78 at (P/e=10) and (e/D= 0.044). [9] studied numerically the forced convection heat transfer with turbulent flow in heat exchanger with spirally semicircle-grooved tube. The results showed that the enhancements on heat transfer highest than the smooth tube is between 1.16–1.96 and on friction loss is 1.2–10.8 times. [10] studied experimentally the heat transfer enhancement by using cross flow finned tube heat exchanger. Showing that the coefficients of heat transfer for finned tube heat exchanger is higher than smooth tube. This present study aims to assess numerically the amount of heat transfer enhancement and pressure drop increasing for a heat exchanger equipped with spirally corrugated tube using one of the available package software CFD and supported by an experimental study. Such a combinations present an important contribution to the field of heat transfer and heat exchangers.

2. Experimental work

2.1 Rig Construction

The design schematic diagram of the test rig is shown in Figure 1, while Figure 2 shows the experimental rig. The test rig is consisting of air duct or wind tunnel having a test section in the middle, constructed from a clear acrylic plastic of (330mm x 330mm x 360mm). The air is supplied by axial ventilation 3 phase motor (Power =2.2 kW). Two water storage tanks are mounted near the wind tunnel to provide uniform hot water to the heat exchanger. Four models of heat exchangers are shown in Figure 3 and Table 1 listed the dimension of these models were designed and fabricated from tubes of copper with thermal conductivity (376W/m. ^{o}C). A number of thermocouples type K were used with 12-chanels data logger (Lutron BTM-4208SD) to measure temperatures at different locations in heat exchanger rig. Along the heat exchanger surface, twelve thermocouples were connected around the pipe to measure the surface temperature of the pipe. In addition, four thermocouples are located in the inlet, middle, and outlet of the heat exchanger. These thermocouples were well calibrated and fixed with glue (Cyanoacrylate adhesive). Digital hot wire anemometer (TES-1341 model) was used to measure the air velocity, while a digital manometer (SDMN6) was employed to measure the pressure difference of air between the inlet and outlet of the test section.

Table 1. Shows the dimension of the various types of heat exchanger. All dimensions (mm)

Heat exchanger	Type	outer diameter (D)	inner diameter	Ribs Pitch(P)	Ribs Pitch angle (Θ^{o})	Ribs width(w)	Ribs depth(h)	P/D	w/D	h/D
Case 1	Plain tube	24	19	-	-	-	-	-	-	-
Case 2	Helical ribs tube	24	19	32	18	12	1.25	1.3	2	0.05
Case 3	Helical ribs tube	24	19	36	27	12	1.25	1.5	2	0.05
Case 4	Helical ribs tube	24	19	44	30	12	1.25	1.8	2	0.05

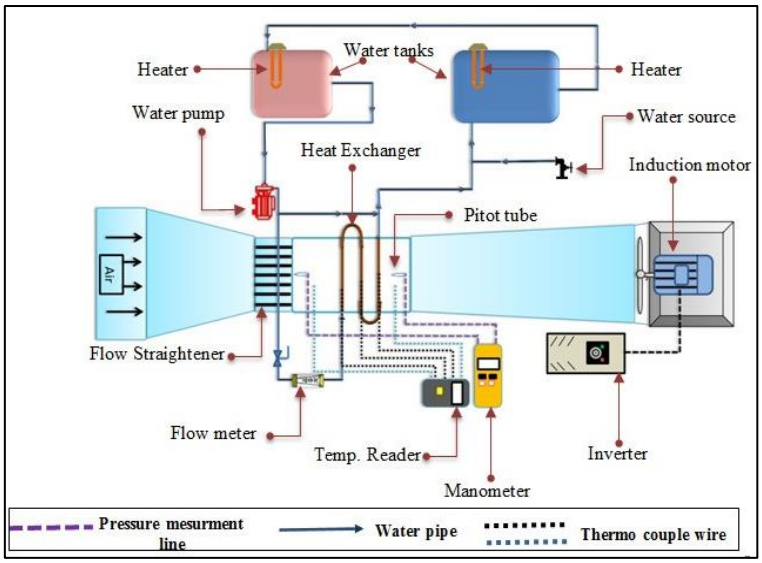

Figure 1. Schematic diagram of experimental set-up.

Figure 2. Experimental setup.

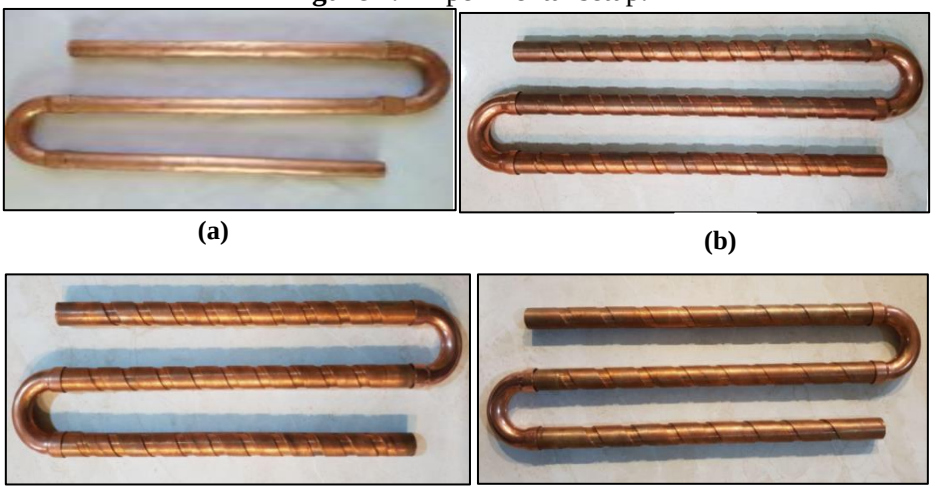

(a) **(b)**

(C) **(d)**

Figure 3. (a) Case 1, (b) Case 2, (c)Case 3, (d) Case 4.

2.2 Experimental Procedure

Four tube heat exchangers models were fabricated and tested, one of them is smooth tube and the three models are helical rib tubes. Six different air speeds are used in the testing for each heat exchanger. Generally, (18) experimental runs were conducted.

The test procedure steps are as follows:

1. The room temperature (T_{room}) is measured and recorded .
2. Switched on the water heater to get water temperature inside the heater tank at the required temperature according to the running experiment.
3. The digital differential manometer, temperature data logger, and hot wire flow meter are switched on.
4. Switched on the axial fan to push the air through the test section while the required airspeed within the test section is adjusted by the inverter selector.
5. Switched on the water pump to pump the water through the heat exchanger tubes.
6. Recording the air inlet and outlet temperatures, tubes wall temperatures, air velocity and water flow rate.

3. Data Analysis

The equation that relates the heat transfer rate that transferred from the hot fluid must be equal to the heat transfer rate that extracted by the cold fluid as follows [11]

$$Q = \dot{m}_a C_{pa}(T_{a,e} - T_{a,i}) = \dot{m}_w C_{pw}(T_{w,e} - T_{w,i}) \quad (1)$$

The heat transfer rate of the isothermal surface given by:

$$Q = h_{av} A_s (T_{s,av} - T_\infty) \quad (2)$$

Then

$$h_{av} = \frac{\dot{m}_w C_{pw}(T_{w,e} - T_{w,i})}{A_s (T_{s,av} - T_\infty)} \quad (3)$$

Cylindrical surface area:

$$A_s = (\pi * D * L_p) \quad (4)$$

$$Nu_{av} = \frac{h_{av} D}{k_a} \quad (5)$$

$$Re = \frac{\rho_a V_{max} D}{\mu_a} \quad (6)$$

For in-line tubes arrangement, the maximum velocity located at the minimum flow area between the tubes as [11]:

$$V_{max} = \frac{S_t}{S_t - D} V \quad (7)$$

The pressure drop can be calculated as follows [11]:

$$\Delta P = f \frac{\rho V_{max}^2}{2} N \quad (8)$$

Here the pressure drop of the airflow across the test heat exchanger models can be expressed as [11]:

$$\Delta P = P_i - P_e \quad (9)$$

Overall enhancement ratio (thermal performance) is defined by the following expression [12], [13];

$$TH = \frac{\frac{Nu}{Nu_\circ}}{\left(\frac{f}{f_\circ}\right)^{\frac{1}{3}}} \quad (10)$$

Based on previous experimental data, several correlation have been proposed to obtain the Nusselt number cross tube banks such as Zukauskas [11] that given by:

$$Nu_{\circ} = 0.86(0.27Re^{0.63}Pr^{0.36}(Pr/Pr_s)^{0.25} \quad (11)$$

In this study, all thermophysical properties evaluated at the arithmetic mean temperature as:

$$T_m = \frac{T_{ai} + T_{ae}}{2} \quad (12)$$

4. Numerical Solution

Three-dimensional air flow and heat transfer across smooth and helical ribs tube heat exchanger was solved by numerical modeling that conducted CFD modeling and simulation software. The post processing and simulation are carried out by ANSYS Fluent 16.2 software [14].

4.1 Computational Domain Geometry

Three dimensional geometrical heat exchanger test section Figure 4 was building by using SOLIDWORKS 2016 x64 Edition software and then it meshed and prepared for simulation by using ANSYS Design Modeler software [14]. The dimensions and specification of considered cases under study were illustrated in Table 2. The Navier-Stokes governing equations of continuity, momentum and the energy conservation equations were solved in three dimensions for the fluid domain (air). The simulation solutions include model properties like air and thermal properties of the solid tubes, model operating conditions and grid boundary conditions must be defined firstly.

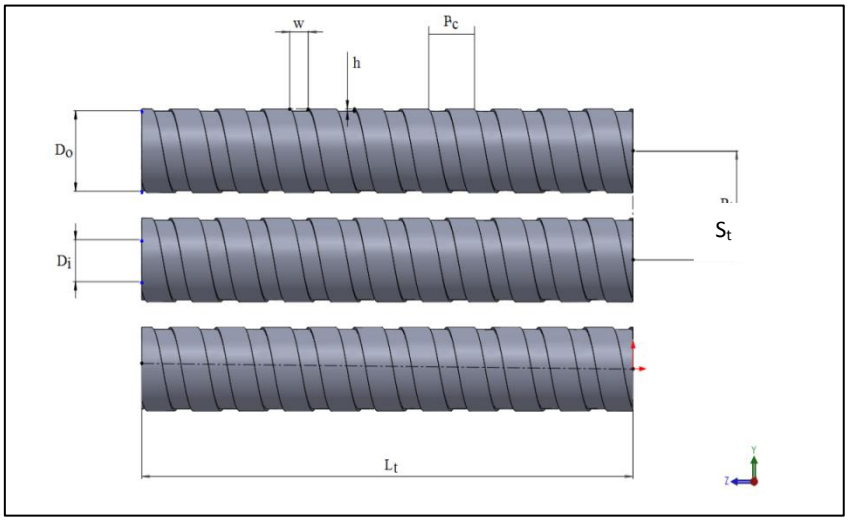

Figure 4. Helical ribs tube heat exchanger**.**

Table 2. The specification and dimensions of considered cases**.**

Parameter	**Symbol**	**Value**
Tubes		
External tubes diameter	*Do*	*24 mm*
Internal tubes diameter	*Di*	*19 mm*
No. of tubes rows	N_t	*3*
Transverse tube pitch	S_t	*65 mm*
Length of tubes	L_t	*330 mm*
Depth of corrugated groove	*h*	*1.25 mm*
Width of corrugated groove	*w*	*12 mm*
Coiled corrugated groove pitch	P_r	*32 mm*

Duct		
Duct width	*W*	*330 mm*
Duct height(Half of it due to symmetry)	*H*	*330 mm*
Duct length	*L*	*360 mm*

4.2 Boundary Conditions

The inlet boundary condition of the heat exchanger test section were analyzed for different air inlet velocities through the duct of 3,5,7,9,11and 13 m/s under the Re range of (7200-31400) at 300 K temperature. The water inlet velocity through the tubes was fixed at 0.12 m/s at 333K temperature. The no slip boundary condition was associated to the outer wall of the heat exchanger helical and smooth tubes and to the duct walls.

4.3 Mesh Generation

For representing and simulating the complex geometry boundaries, the tetrahedral mesh elements are more flexible in use [14]. Five mesh element types was used to study the mesh independence as lists in Table 3. A independency of mesh test was presented by varying the number of elements from 217126 to 850000, also the meshing of smooth and helical ribs is shown in Figue 5.

Table 3. Dependency of the present mesh results.

No	Number of nodes	Tip temperature(ºC)	Duct pressure drop (Pa)
a	217126	328.4798	115.1681
b	376010	330.849	104.5633
c	534894	333.8798	85.6
d	693778	334.9	83.35389
e	852662	335.1	82.6

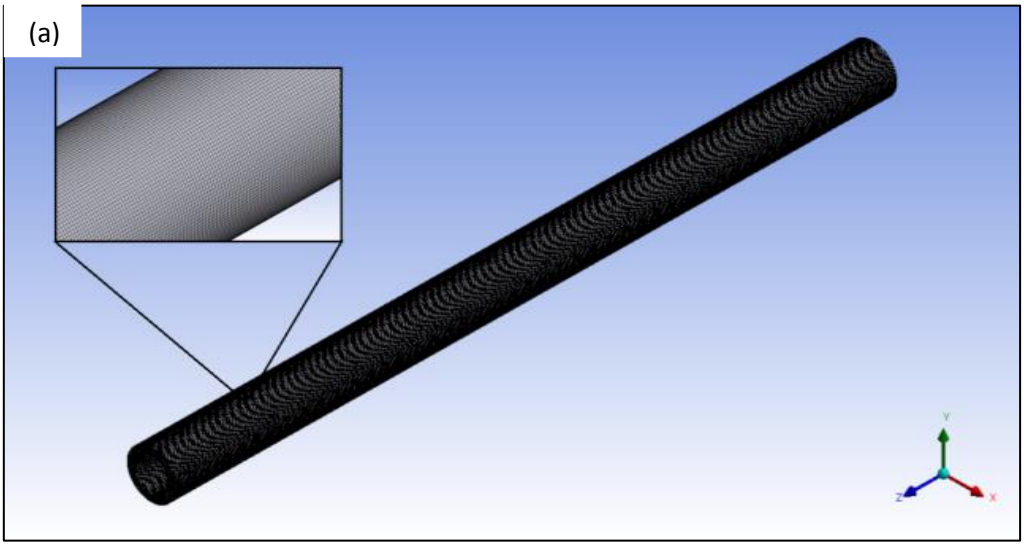

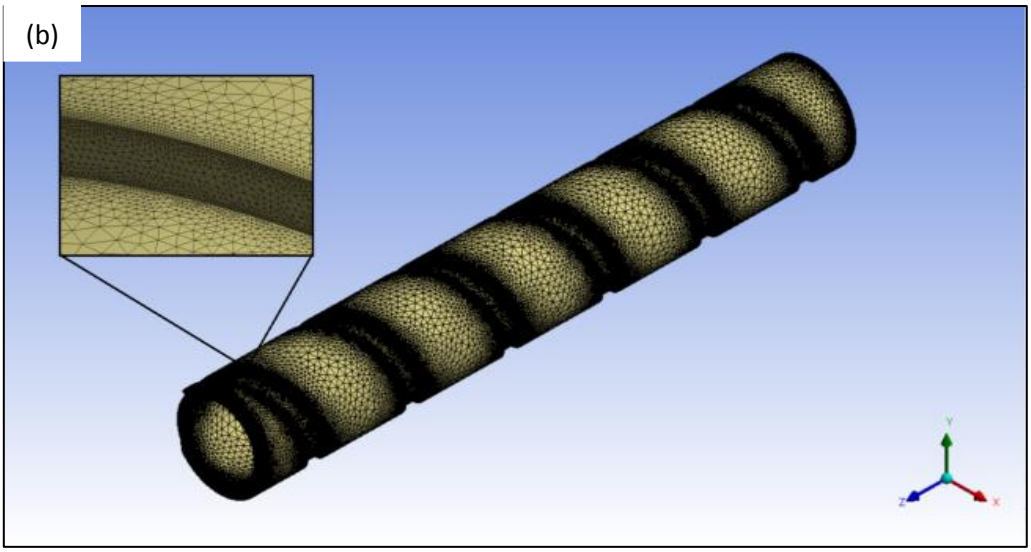

Figure 5. Mesh of tube (a) smooth (b) Helical ribs**.**

5. Results and discussion

The effects of the helical ribs tube with a different shape variables (rib pitch to diameter ratios (P/D=1.3, 1.5 and 1.8), with a ratio of rib height to diameter of (h/D=0.05) and a ratio of rib width to diameter of (w/D=2)) under Re=7200 to 31,400 range on the friction factor and also the heat transfer are presented in this section. The experimental data of friction factor and Nusselt number of the smooth tube are validated with the results of equations of Zukauskas [11]. The comparisons of friction factor and Nusselt number are shown in Figures (6 and 7). The results showed a good agreement for smooth tube with deviations of ±3% in Nusselt number and ±30% for friction factor. This deviation was referred to the surface pipe roughness, since Zukauskas equation was developed for smooth pipe.

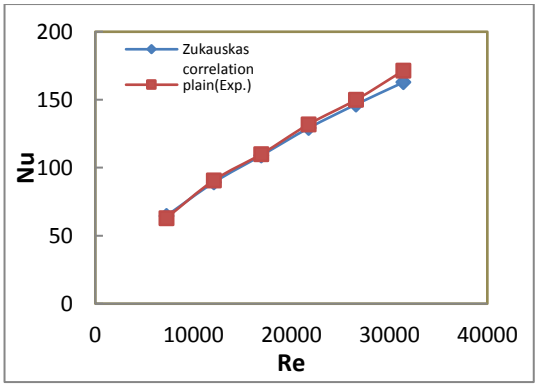

Figure 6. Nusselt number Validation of the plain tube**.**

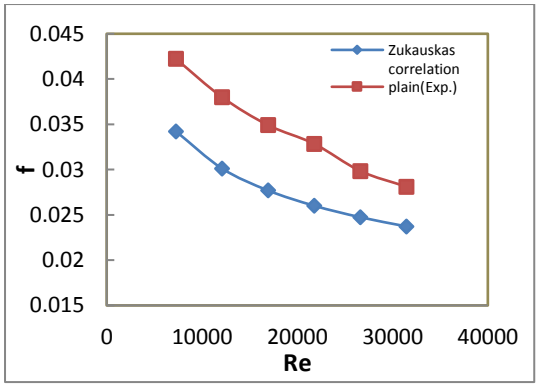

Figure 7. Friction factor Validation of the plain tube.

Figure 8 shows a comparison between the values of Nusselt number and Reynolds number of the helical ribs tubes with the smooth tube. In the helical ribs tube case with a pitch ratio of (P/D=1.8), the Nusselt number increases by 53% over the smooth tube and by 37% and 31%, when using P/D=1.5 and 1.3 respectively. It is interesting to note that the Nusselt number increases with increasing the pitch ratio value, in other side; the enhancement of heat transfer increase when the severity index increase [15]. Figure 9 shows that the increasing Reynolds number will lead to decreasing the friction factor in the helical ribs tube gradually. In addition, the friction factor of smooth tube was less than the helical ribs tubes due to high viscosity losses near the tube wall from helical ribs surfaces. This leads to dissipate the dynamic pressure of the fluid and caused by the re-circulating and turbulence flows.

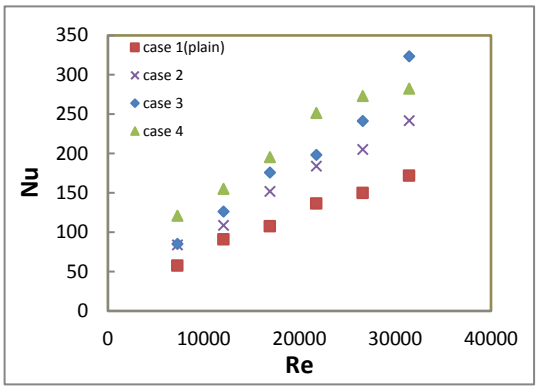

Figure 8. Comparison between Nusselt number for all Present Cases and plain tube for the present experimental results.

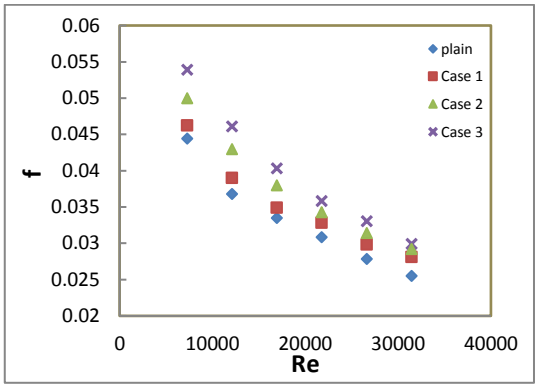

Figure 9. Comparison between frication factor for all Present cases and plain tube for the present experimental results.

Thermal performance factor (η) calculated according to equation (10) of the helical ribs tube with highest pitch ratios is presented in Figure 10, which shows that the performance factor increases with the rise of pitch ratio and the performance factor tends to decrease as the Reynolds number increases. The maximum thermal performances of (P/D) = 1.8 found to be 37.5%, which is the highest than the other cases.

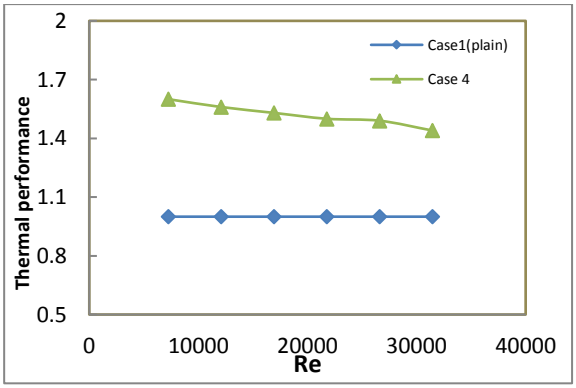

Figure 10. Comparison between thermal performances for case 4 (P/D=1.8), and plain tube for the present experimental results.

Figure 11 and Figure 12 are compared between the Nusselt number of the numerical and experimental results. The numerical results give a good agreement with the present experimental results, the deviation in Figure 11 is 12% and Figure 12 is 11% higher for numerical as an average value. Figure 13 and Figure 14 reveals the comparison between the numerical and experimental results of friction factor for present cases. The deviation in Figure 13 is 6% and Figure 14 is 9% higher for experimental as an average value.

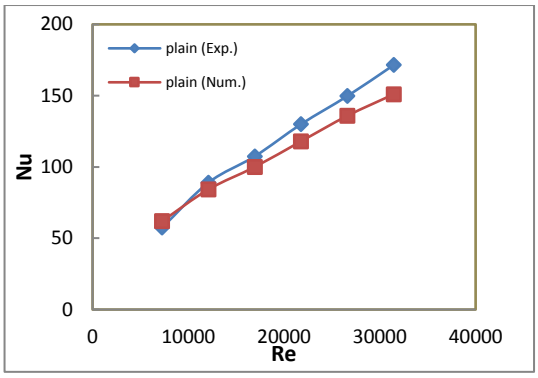

Figure 11. Comparison between the numerical & experimental results of Nusselt number for present plain.

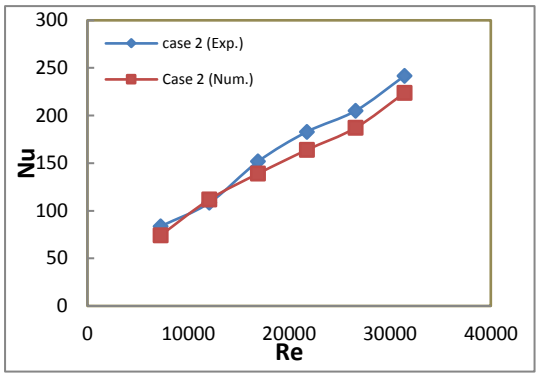

Figure 12. Comparison between the numerical & experimental results of Nusselt for present case2.

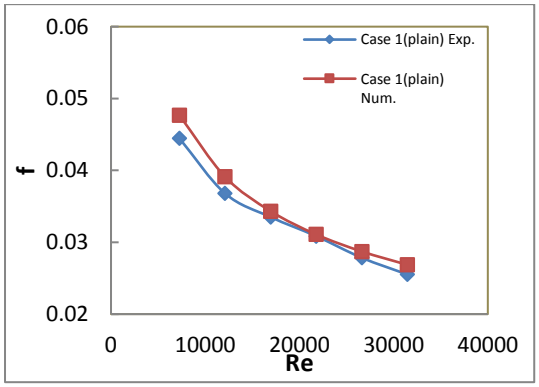

Figure 13. Comparison between the numerical & experimental results of frication factor for present plain.

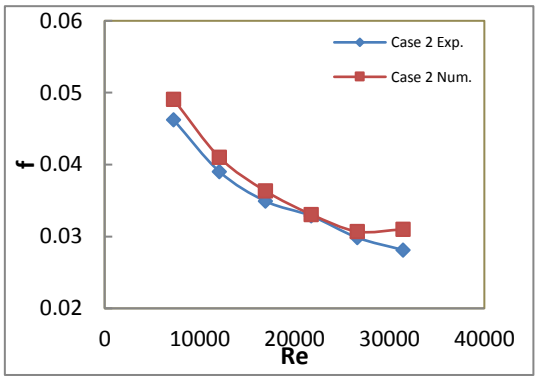

Figure 14. Comparison between the numerical & experimental results of frication factor for present case2.

Figure 15 shows a 2-D projection velocity contour for fluid flow simulated for two heat exchanger cases under the inlet velocity 3 m/s. A comparative evaluation of the vortices made for the plain and ribs tube, illustrating clearly the causes of the ribs on the surface of the tube that lead to increase the velocity near the wall for ribs tubes, which making the flow become more turbulent.

Figure 16 shows the temperature distribution contour for the two models of heat exchanger under inlet air flow velocity 3 m/s. For this present analysis inlet air temperature was kept constant at 25 °C, the inner wall temperature of heat exchanger was 60 °C and outlet air pressure was assumed to be zero. It is clear that helical ribs have been introduced to the surface of the tube which causes vortices near the wall of the tube, which is attempting to improve the flow characteristics and further promote heat transfer.

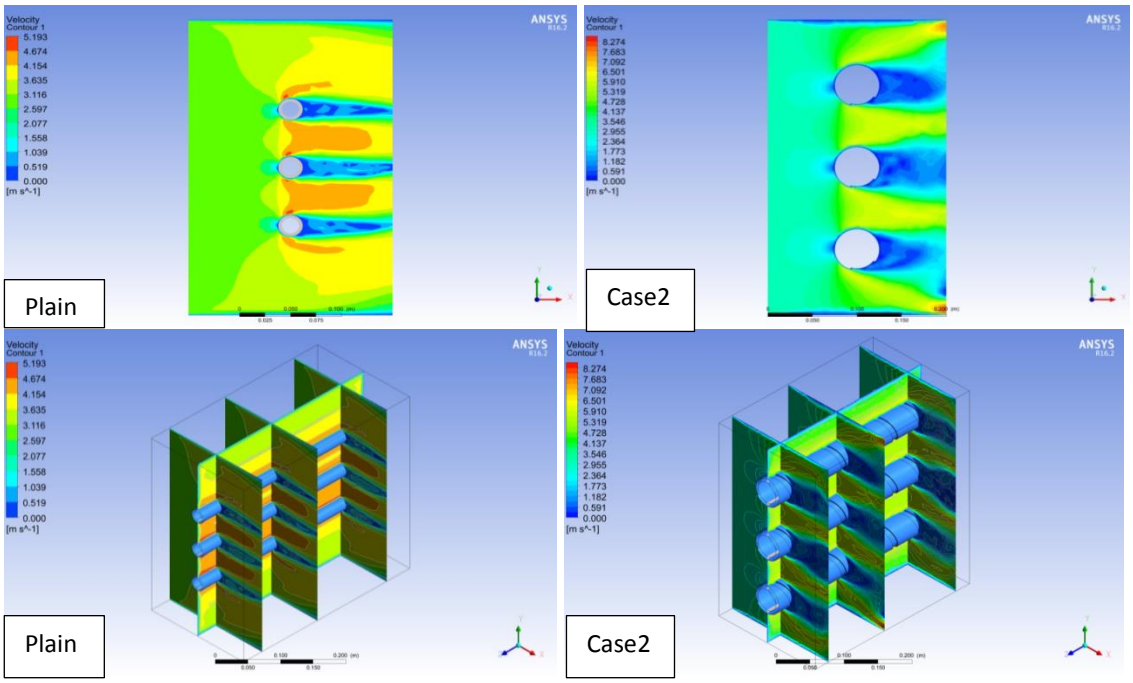

Figure 15. 2-D & 3-D velocity contour projection for plain & case(2) model at 3 m/s inlet velocity.

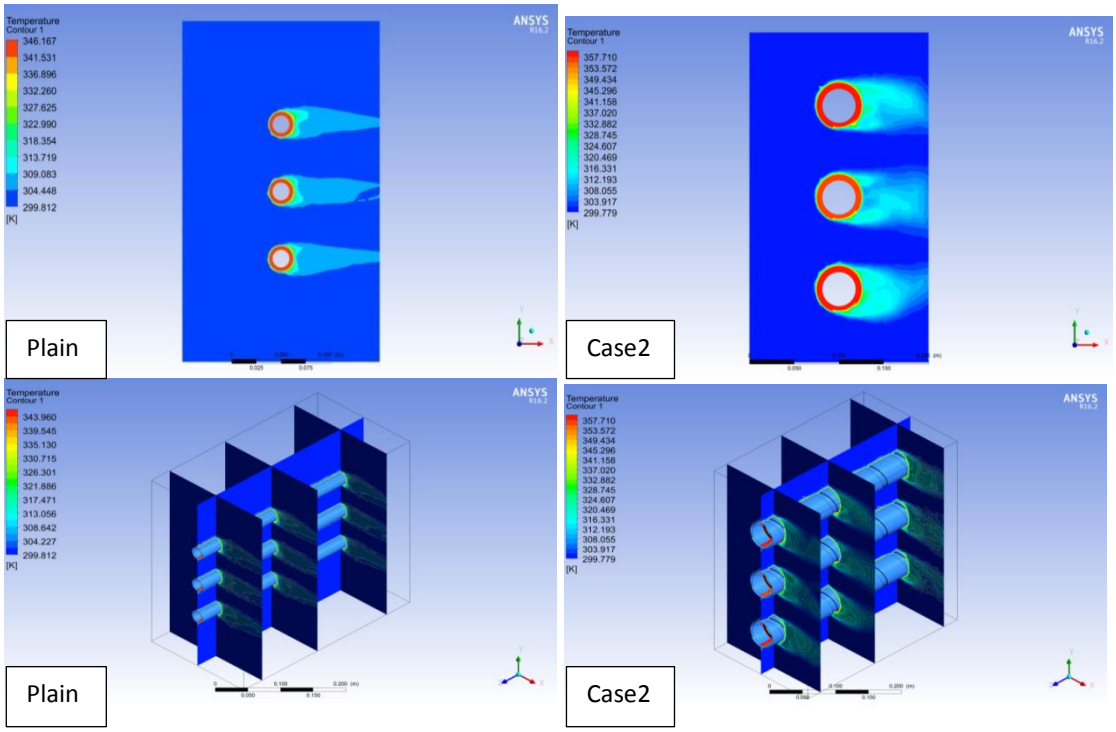

Figure 16. 2-D & 3-D temperature contour for plain & case2 model at 3 m/s inlet velocity& 5000 W/m^2 heat flux.

6. Conclusion:

The present numerical and experimental results that given from the resent work will present the following conclusion:

1) The average Nusselt number increases with increasing the air inlet Reynolds number for the two models of smooth and ribs helical heat exchanger.
2) The friction factor decreases with increasing the air inlet Reynolds number.
3) There is a good enhancement was obtained by using helical ribs tube heat exchanger as relative to smooth tube heat exchanger.
4) There is a good agreement between the experimental and numerical results in the present results.
5) For the ribbed tubes, Nusselt number obtained up to 53% for (P/D) =1.8, 37% for (P/D) =1.5 and 31% for (P/D) =1.3, in comparison with the smooth tube.
6) In case 4 of (P/D) =1.8 gives the highest thermal performance than other cases.

References:

[1] Johar G and Hasda V 2010 *Experimental Studies on Heat Transfer Augmentation Using Modified Reduced Width Twisted Tapes (RWTT) as Inserts for Tube Side Flow of Liquids* Department of Chemical Engineering National Institute of Technology Rourkela.
[2] Mahureand A and Kriplani V 2012 *International Journal of Engineering* **5** 241-249.
[3] Veysel O zceyhan and Necdet Altuntop 2005 *Heat transfer and thermal stress analysis in grooved tubes*.
[4] Bilen K, Cetin M, Gul H and Balta T 2009 *Applied Thermal Engineering* **29** 753–761.
[5] Pethkool S, Eiamsa-ard S, Kwankaomeng S and Promvonge P 2010 Turbulent heat transfer enhancement in a heat exchanger using helically corrugated tube.
[6] Hossainpour S and Hassanzadeh R 2011 *International Journal of Energy and Environmental Engineering*.
[7] Pitak Promthaisong, Withada Jedsadaratanachai and Smith Eiamsa-ard 2011 Numerical simulation and optimization of enhanced heat transfer in helical oval tubes: Effect of helical oval tube modification, pitch ratio and depth ratio.
[8] Pawan Singh Kathait and Anil Kumar Patil 2014 Thermo-hydraulic performance of a heat exchanger tube with discrete corrugations.
[9] Pitak P, Amnart B and Withada J 2016 *International Journal of Mechanical and Materials Engineering*.
[10] Zena K. Kadhim, Muna S. Kassim and Adel Y. Abdul Hassan 2016 *International Journal of Computer Application* **139** 0975 – 8887.
[11] Gengel YA 2003 *Heat Transfer: A Practical Approach Second Edition* McGraw-Hill.
[12] Adrian Bejan and Allan D. Kraus 2003 *Heat Transfer Handbook*.
[13] Nabil J. Yasin and Mahmood H. Oudah 2018 *International Journal of Energy Engineering* **8** 120-18.
[14] FLUENT 2006 *FLUENT 5 User's Guide* Fluent Inc. Lebanon New Hampshire.
[15] Ghassan F. Smaisim 2017 *Al-Qadisiyah Journal For Engineering Sciences* **10** 1998-4456.

Nomenclatures:

A cross-sectional area (m^2)
As Tube surface area (m^2)
Cp Specific heat at constant pressure (J/kg.K)
D Tube diameter (m)
S_t Distance between tubes.
N Number of tube
L_p Test section length (m)
f_o Friction factor
V Air velocity (m/s)
h_{av} Average heat transfer coefficient (W/ m^2.K)
$\dot{m}$ Mass flow rate (kg/s)
Re Reynolds number
Nu_o Average Nusselt number

P Pressure (pa)
Pr Prandtl number
K Thermal conductivity (W/m.K)
Q The rate of heat transfer (W)
T Temperature (C, K)
μ_a Dynamic Viscosity (kg/m.s)
ρ Variable Density (kg/m^3)
ΔP Pressure Drop (Pa)
TH Thermal Performance